Chapter 7 Aircraft Flotation Analysis

7.1. Introduction

The configuration of the landing gear has a direct impact on ground flotation, a term used to describe the capability of pavement and other surfaces to support an aircraft [32]. The number and arrangement of the wheels, along with the aircraft weight and its distribution between the nose and main assemblies, dictates the required pavement thickness for a particular aircraft. In addition, the type of the pavement found at the airports to be served by the aircraft also need to be considered. As shown in Fig. 7.1, existing runway and apron pavements can be grouped into two categories: flexible and rigid [7]. A flexible pavement, more commonly known as asphalt, may consist of one or more layers of bituminous materials and aggregate, *i.e.*, surface, base, and subbase courses, resting on a prepared subgrade layer. On the other hand, rigid pavement may consist of a slab of portland cement concrete placed on a layer of prepared soil. The thickness of each of the layers must be adequate to ensure that the applied loads will not damage the surface or the underlying layers.

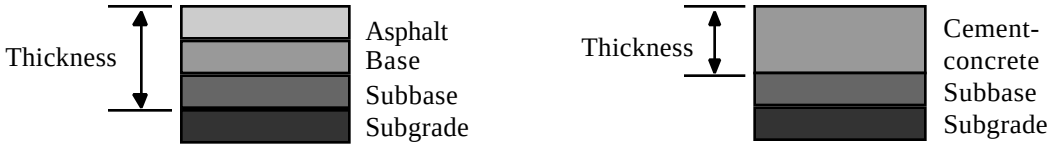

a) Flexible pavements b) Rigid pavements

Figure 7.1 Theoretical pavement cross-sections [33]

Based on the analyses as outlined in this chapter, a program was developed to determine the required flexible and rigid pavement thickness for a particular aircraft. Results obtained from the program were validated with actual design data to ensure that a high degree of reliability can be placed upon the program itself.

7.2. Design Pavement Thickness

Various flotation analyses have been developed over time in different countries and by different government agencies and organizations. Some agencies and organizations and the corresponding design methods are listed as follows [7]: the Federal Aviation Administration (FAA), the Portland Cement Association (PCA), the Waterways Experiment Station (S-77-1), and the British Air Ministry (LCN). The majority of these methods use the California bearing ratio (CBR) method of design for flexible pavements and Westergaard stress analysis for the rigid pavements [7].

7.2.1. Flexible Pavements

For flexible pavements, CBR is the standard measurement used to classify the bearing strength of the subgrade. It is essentially the ratio of the bearing strength of a given soil sample to that of crushed limestone gravel. It is expressed as a percentage of the limestone figure, *i.e.,* a CBR of ten means that the subgrade has a bearing strength of ten percent to that of crushed aggregate. The original design method, which was developed by the California Division of Highways in 1928, evaluates the pavement thickness requirements for a given load condition and soil strength, assuming that the load is carried on a single wheel with a circular footprint area.

Until the middle of the 1950s, the analysis developed for the B-29, which features a dual wheel configuration, was extended to develop thickness design relationships for new aircraft with twin-tandem configurations. However, it appears that the analysis tends to produce slightly unconservative thickness estimates. Subsequent reevaluation of the theoretical work, which is based on Boussinesq's theory [5], and test data showed that the slopes of pavement deflection versus wheel offset for the single wheel were equal to or steeper than for dual wheels at equal depths, as shown here in Fig. 7.2. A direct result of this study is the introduction of the concept of the equivalent single-wheel load (*ESWL*), which eventually became the foundation of the S-77-1 design method [34 and 35]. *ESWL* is essentially a fictitious load on a isolated wheel, having the same inflation pressure, and causing the same stresses in the runway material as those due to a group of wheels. This fictitious wheel load accounts for the fact that a given loading, spread over a number of contact areas, causes lower stresses in the runway material than would be the case when the same load is concentrated on a single wheel.

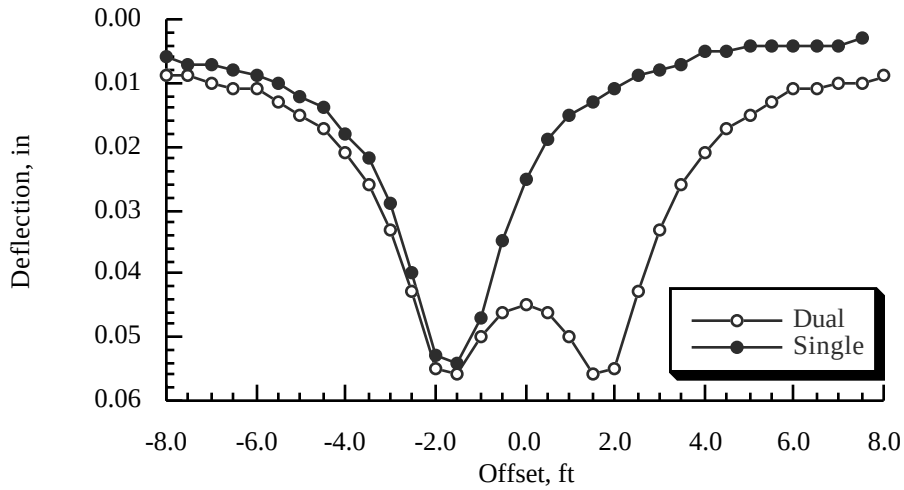

Figure 7.2 Comparison of single- and dual-deflection profiles, 1.0-foot depth [7]

Probable locations where maximum pavement bearing stress might occur, *e.g.*, directly under and between the tire contact areas, are shown in Fig. 7.3, The offset distance between these points and the center of individual tire contact area, as well as the depths below the surface at which the *ESWL* is computed, which is treated as the thickness of the pavement in the analysis, are subsequently represented in terms of the radius of the footprint area (r) [7, p. 429]

$$r = \sqrt{\frac{A}{\pi}} \tag{7.1}$$

and the tire-ground contact area (A) is defined as

$$A = \frac{F}{P} \tag{7.2}$$

where F is the vertical main assembly load (per strut) and P is the tire inflation pressure.

Given the offset distances and depths, curves such as the ones shown in Fig. 7.4 are used to determine the corresponding deflection factors. The principle of superposition is then used in calculating the multiple-wheel deflection factor (f), which is equal to the summation of the deflection factors produced by each tire in the multiple-wheel assembly at the point of analysis.

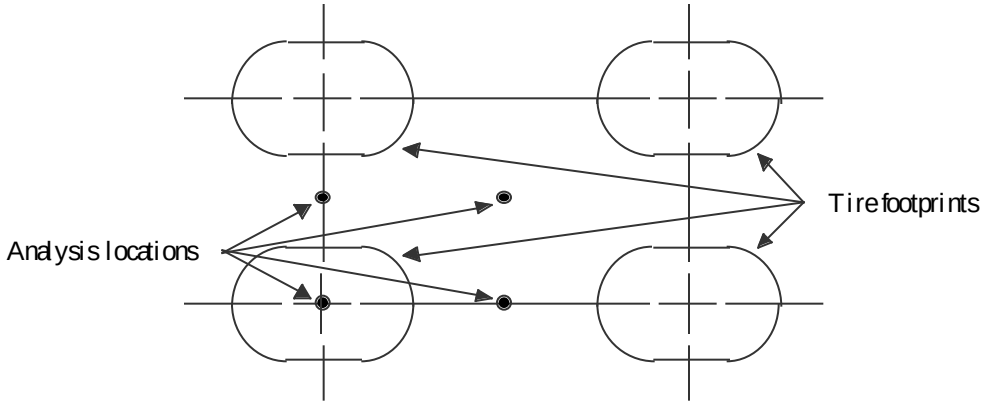

Figure 7.3 Relationship between the tire-contact areas and the analysis locations

The ratio of load intensity of the single-wheel configuration to a single wheel of the multiple-wheel configuration is defined as the inverse of the ratio of the maximum deflection factors at a given depth, *i.e.*, the pavement thickness, [7, p. 430]

$$\frac{F_s}{F_m} = \frac{f_m}{f_s} \tag{7.3}$$

where subscripts s and m denote single- and multiple-wheel configurations, respectively. Once the ratio of load intensity is determined, the *ESWL* is calculated using the expression

$$ESWL = \frac{F_s F}{F_m N_w} \tag{7.4}$$

where N_w is the number of wheels per strut. To account for the loading effect caused by the number of annual aircraft operations, the design thickness (t) corresponding to a given CBR value is estimated using the expression [7, p. 433]

$$t = \alpha_i \sqrt{\frac{ESWL}{8.1CBR} - \frac{A}{\pi}} \tag{7.5}$$

where α_i is the load repetition factor as shown in Fig. 7.5. It is categorized by the number of tires used to calculate the *ESWL* and typically value corresponding to 10,000 passes are used in the calculation [33].

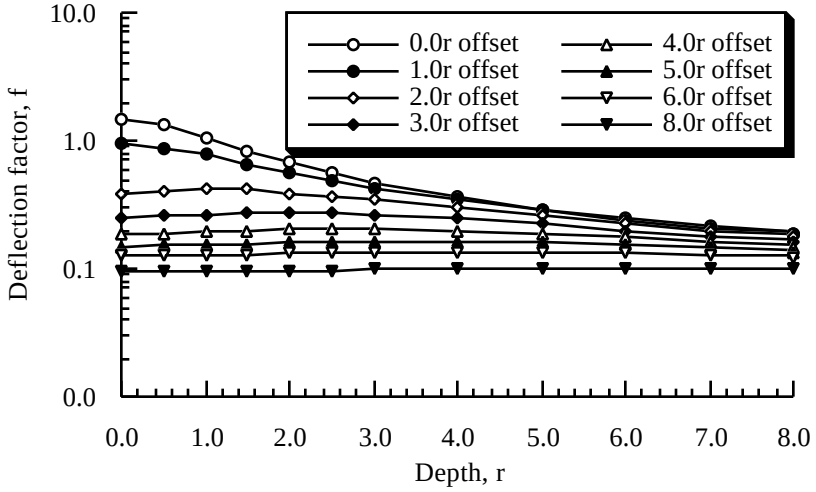

Figure 7.4 Deflection factor curves for Poisson's ratio of 0.5 [34]

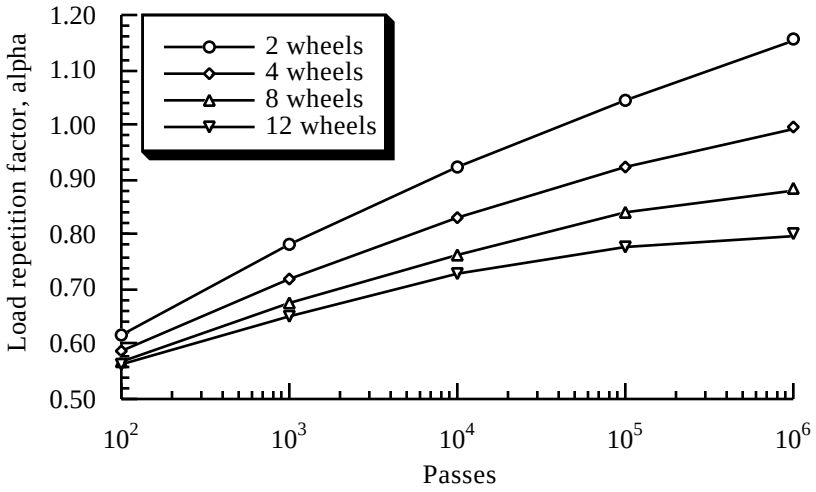

Figure 7.5 Aircraft load repetition factor [7]

7.2.2. Rigid Pavements

Stress in a concrete pavement is induced in four ways: tire loads, change of shape of slab due to differential in temperature and moisture between the top and the bottom of the slab, and the friction developed between slab and foundation when the slab expands/contracts. Since the primary consideration in the design of any pavement is the load which it is to carry, only the stresses induced by tire loads will be addressed.

The Westergaard stress analysis [36] assumes that the slab is a homogeneous, isotropic, and elastic solid in equilibrium. The reactions of the subgrade are assumed to be in the vertical direction only, and is proportional to the deflections of the slab. Additionally, the wheel load is assumed to be distributed over an elliptical footprint area. The stiffness of the slab relative to that of the subgrade is represented by the radius of relative stiffness of the concrete (l) [37, p. 56]

$$l = \sqrt[4]{\frac{Ed^3}{12\left(1-\mu^2\right)k}} \tag{7.6}$$

where E is the modulus of elasticity for the concrete, d is the thickness of the slab, μ is the Poisson's ratio for the concrete, and k is the modulus of subgrade reaction. Typically, E is taken as 4,000,000 psi and μ as 0.15 [7].

Critical bearing stresses for the interior and edge loading cases are examined. For the interior loading case, the load is applied at the interior of the slab at a considerable distance from any edge or joint. The maximum tensile stress (σ) at the bottom of the slab is given as [7, p. 441]

$$\sigma_{int} = \frac{F_s}{d^2}\left\{0.275(1+\mu)log_{10}\frac{Ed^3}{k\left[(a+b)/2\right]^4} + 0.293(1-\mu)\frac{a-b}{a+b}\right\} \tag{7.7}$$

where F_s is the single wheel load, d is the design thickness, and a and b are the semi-axes of the footprint area ellipse. Considering the edge loading case next, the load is applied adjacent to an edge that has no capacity for load transfer. The maximum tensile stress is given as [7, p. 442]

$$\sigma_{ext} = \frac{2.2(1+\mu)F_s}{(3+\mu)d^2} log_{10} \frac{Ed^3}{100k[(a+b)/2]^4} + \frac{3(1+\mu)F}{\pi(3+\mu)d^2}\left[1.84 - \frac{4}{3}\mu + (1+\mu)\frac{a-b}{a+b} + 2(1-\mu)\frac{ab}{(a+b)^2} + 1.18(1+2\mu)\frac{b}{l}\right] \quad (7.8)$$

Although the edge loading case produces a maximum stress that is the more critical of the two cases, in reality the probability of occurrence of this type of loading is relatively small, *i.e.*, the traffic tends to be channelized with the highest concentration in the vicinity of the runway and taxiway centerlines [7]. In addition, rigid pavement design charts as provided by PCA, which are used as reference data in the following section, are based on the interior loading case. Therefore, the interior loading condition is selected as the basis of the rigid pavement analysis.

7.3. Pavement Thickness Estimates

Design pavement thickness and corresponding ACNs for the Boeing Models 737, 747, 767, and McDonnell Douglas DC10 were determined for four subgrade strength categories: ultra-low, low, medium, and high [33]. Each category is assigned a CBR value for the flexible pavements and a *k* value for the rigid pavements; numerical values of each category are listed in Table 7.1.

Table 7.1 Subgrade strength categories [33]

Category	**CBR**	***k*, lb/in^3**
Ultra-low	3.0	75.0
Low	6.0	150.0
Medium	10.0	300.0
High	15.0	550.0

For flexible pavements, *ESWL*s were computed using Eq. (7.4) from the surface down in multiples of footprint area radius. At each analysis depth, a CBR value was calculated using Eq. (7.5) and the repetition factor corresponding to 10,000 aircraft passes [33]. The result of this calculation is a set of design thickness and CBRs. Linear interpolation is then used to determine the final design thickness corresponding to the subgrade strength CBR values.

For rigid pavements, *l*s were computed using Eq (7.6) from the surface down in predetermined increments, *i.e.*, the design thickness, for each of four subgrade categories. At each design thickness and *k* value, a maximum tensile stress was calculated using Eq. (7.7). The result of this calculation is four sets of design thickness and the corresponding stresses. Linear interpolation is then used to determine the final design thickness corresponding to a concrete working stress of 400 psi [2].

Actual [7, 22, 38, and 39] and estimated pavement thickness are compared to determine the reliability of both analyses. As shown in Fig. 7.6a, the S-77-1 method tends to underestimate the required pavement thickness at the lower end of the CBR range, while it tends to overestimate the required pavement thickness at the upper end of the CBR range. Yet, the trend is consistent with the results obtained from a number of full-scale test tracks, *i.e.*, for heavy wheel loads, the theoretical thickness appeared to be too low for lower CBR values, and too high for higher CBR values. An interesting trend is observed upon closer examination of the actual pavement thickness data. As the subgrade strength increases, the required pavement thickness for aircraft with dual-twin truck assembly configurations, *i.e.*, B747, B767, and DC10, approach, if not fall below, the one required by aircraft with twin-wheel configuration, *i.e*., B737. This can be attributed to the fact that the load on the pavement is better distributed as the number of wheels per assembly increases.

A vastly different trend, as shown in Fig. 7.6b, is exhibited by the Westergaard stress analysis: it tends to underestimate the required pavement thickness by roughly 30 percent across the entire *k* range. The discrepancy can be attributed to the simplicity of the analysis itself. Primarily, the analysis did not consider the variations in the location and direction of maximum moment and stress in the concrete slab [37]. Essentially, the position of the maximum stress can be shifted and rotated depending on the magnitude of *l* and the configuration and dimension of the truck assembly. In addition, the analysis did not include detailed design parameters such as fatigue of concrete due to repeated loading and interactions between layers of materials.

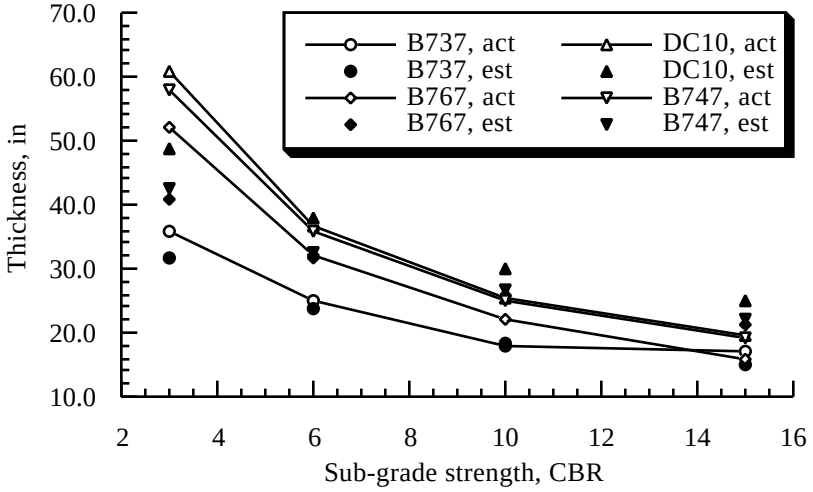

a) Flexible pavements

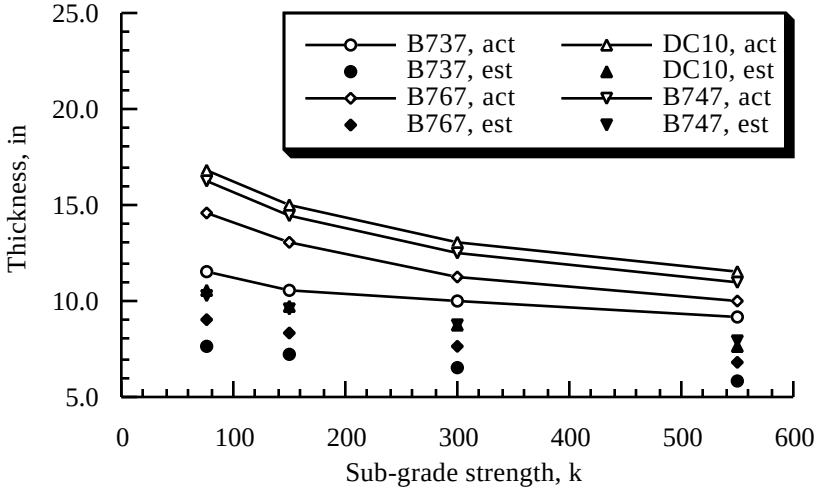

b) Rigid pavements

Figure 7.6 Actual and estimated pavement thickness comparison

Linear regression analysis was used to calibrate the estimated pavement thickness (t_{est}) against actual data. At each subgrade strength category, an aircraft weight-based correction factor is calculated using the expression

$$f_c = c_1 W + c_c \tag{7.9}$$

where c_1 and c_2 are constant coefficients as listed in Table 7.2. The estimated value and correction factor are then combined to arrive at the calibrated pavement thickness (t_{cal}), that is,

$$t_{cal} = t_{est} + f_c \tag{7.10}$$

The objective of this effort is to ensure that the discrepancy between the actual and estimated values will remain within a tolerable range. This is important when both analyses are used to examine the flotation characteristics of aircraft that are outside the existing pavement thickness database, namely, the next-generation high capacity commercial transports. As shown in Fig. 7.7, the calibrated thickness compared reasonably with the actual data.

Table 7.2 Pavement thickness correction constants

	c_1	c_2
Flexible		
Ultra-low	0.000017	3.726
Low	0.000002	0.198
Medium	-0.000002	-1.630
High	-0.000007	-0.008
Rigid		
Ultra-low	0.000003	4.002
Low	0.000003	3.420
Medium	0.000001	3.407
High	0.000000	3.325

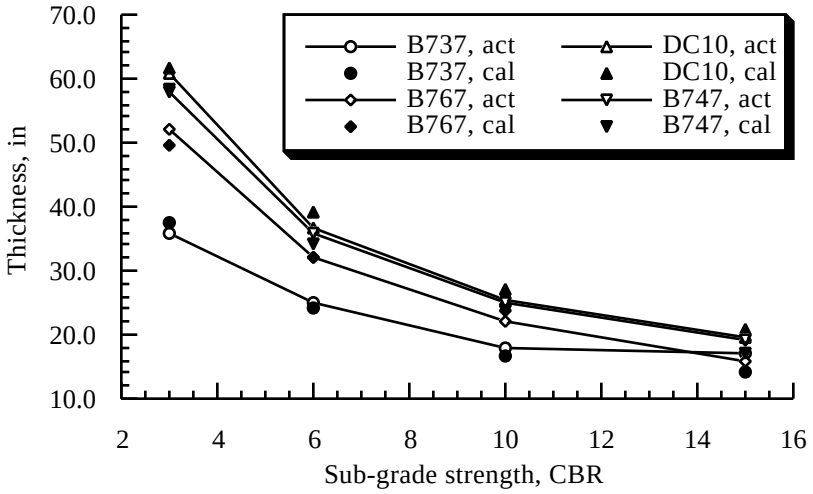

a) Flexible pavements

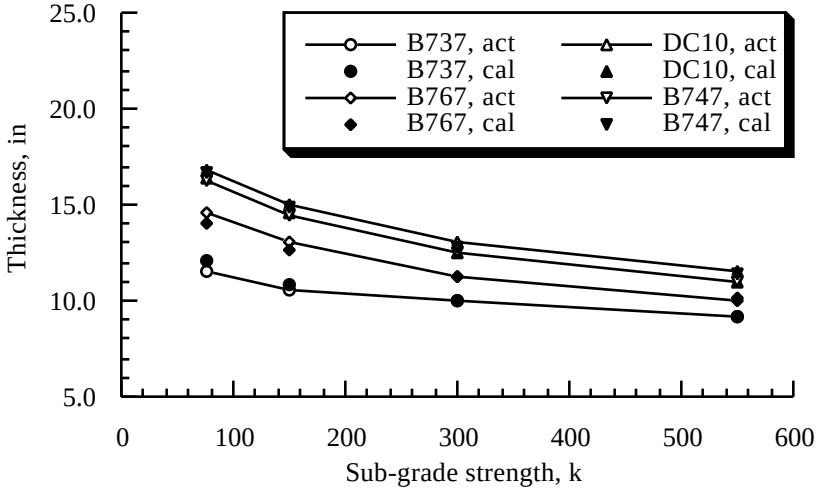

b) Rigid pavements

Figure 7.7 Actual and calibrated pavement thickness comparison

7.4. ACN-PCN Conversion

In an effort to resolve the difference among various pavement design and evaluation methods, the International Civil Aviation Organization (ICAO) recommended universal adoption of the Aircraft-Pavement Classification Number (ACN-PCN) system [39] in 1983. The ACN-PCN system is not intended for the design or evaluation of pavements. It is, instead, a convenient and simple way of categorizing and reporting the pavement's capability to support aircraft on an unrestricted basis. The major appeal of the system is that it allows aircraft manufacturers to use any design/evaluation method of choice to determine the pavement thickness requirements of a particular aircraft. The design thickness is then converted to ACN and compared to PCNs of the airports to be served. If the ACN is equal to or less than the PCNs, the aircraft is cleared to operate out of the given airports subject to any limitation on the tire pressure.

The flexible pavement ACN is calculated using the expression [33, p. 3-11]

$$ACN = \frac{\left(t^2 / 1000\right)}{(0.878 / CBR - 0.01249)} \tag{7.10}$$

where the design thickness t is expressed in terms of centimeters. As for the rigid pavements, ACN is obtained using the conversion chart as shown in Fig. 7.8.

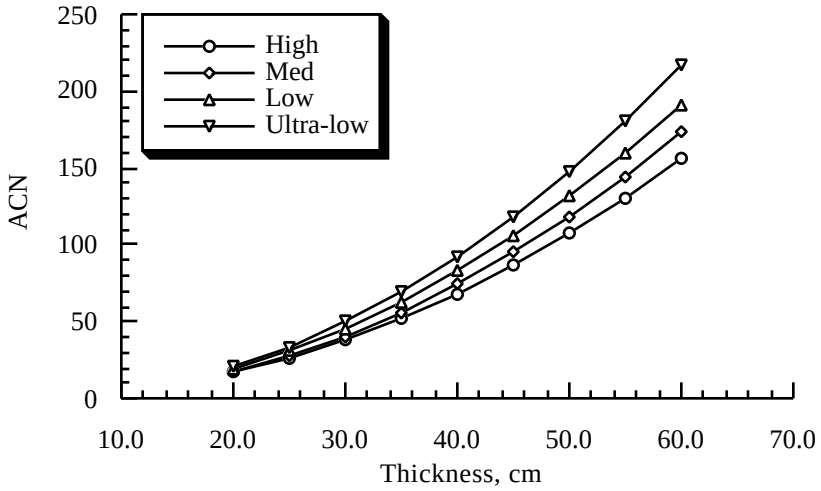

Figure 7.8 Rigid pavement ACN conversion chart [33]

7.4.1. ACN Estimates

Flexible and rigid pavement thickness requirements obtained earlier were converted to ACNs for conversion validation purposes. As shown in Fig. 7.9a, the estimated flexible pavement ACNs exhibit a trend similar to that of the thickness estimates, *i.e.,* too low for lower CBR values and too high for higher CBR values. Apparently, the thickness calibration process did not eliminate the discrepancy introduced in the pavement thickness calculation entirely, and that the trend is carried over into the ACN conversion process. On the other hand, it appears that the calibration process for the rigid pavement has removed most of discrepancy that was introduced in the pavement thickness calculation. As shown in Fig. 7.9b, the conversion, in fact, overestimated the ACN for all aircraft across the entire *k* range.

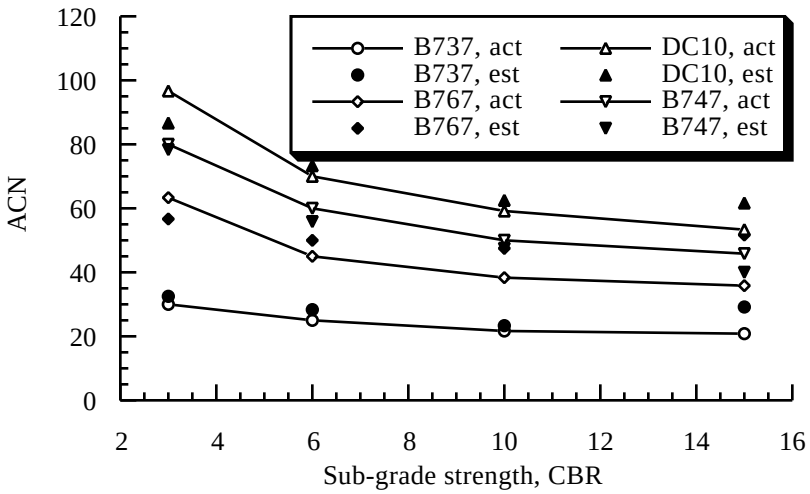

a) Flexible pavements

Figure 7.9 Actual and estimated ACN comparison

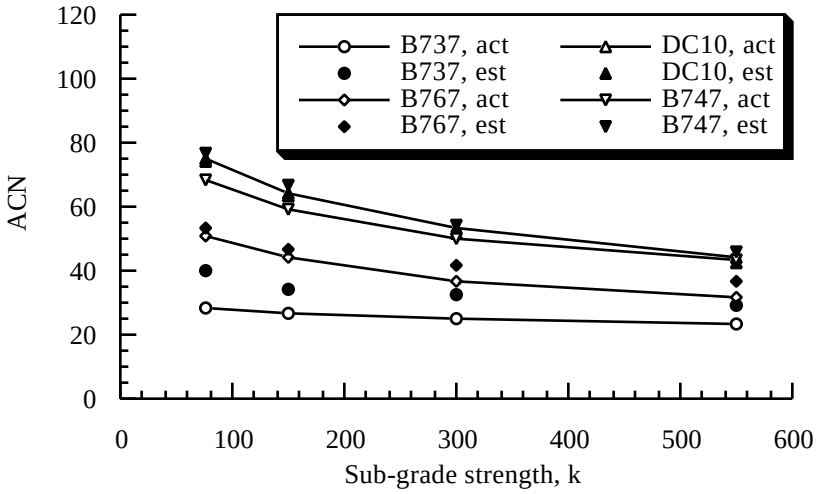

b) Rigid pavements

Figure 7.9 Actual and estimated ACN comparison (concluded)

Linear regression analysis was again used to calibrate the estimated ACN (ACN_{est}) against actual data. At each subgrade strength category, an aircraft weight-based correction factor is calculated using Eq. (7.9), except in this case the constant coefficients are c_3 and c_4 as listed in Table 7.3, The estimated value and correction factor are then combined to arrive at the calibrated ACN (ACN_{cal}), that is,

$$ACN_{cal} = ACN_{est} + f_c \tag{7.11}$$

As shown in Fig. 7.10, the calibration process has successfully brought the estimated ACNs closer to the actual data and thus improved the reliability of the flotation analysis.

Table 7.3 ACN correction constants

	c_3	c_4
Flexible		
Ultra-low	0.000008	0.5178
Low	0.000010	-6.326
Medium	0.000009	-6.769
High	0.000022	-16.182
Rigid		
Ultra-low	0.000006	-8.245
Low	0.000002	-4.940
Medium	0.000009	-7.628
High	0.000008	-6.519

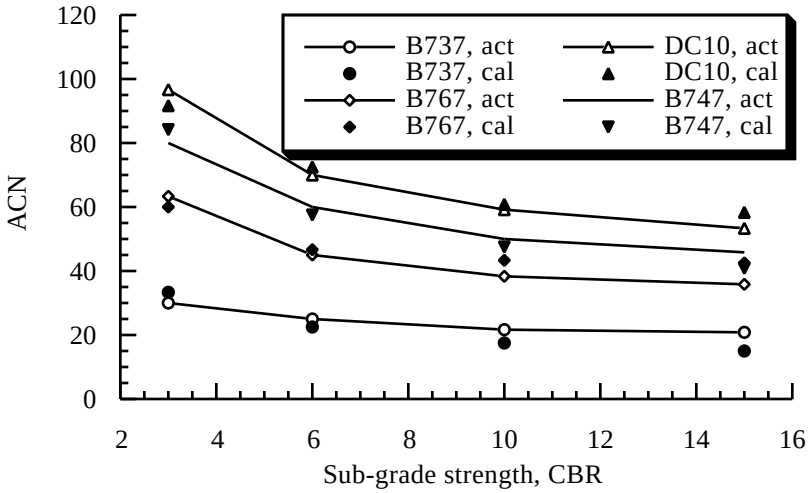

a) Flexible pavements

Figure 7.9 Actual and calibrated ACN comparison

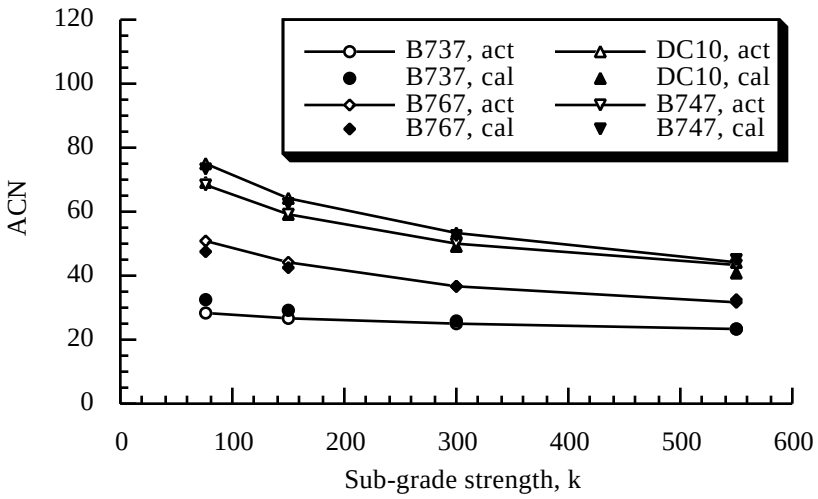

b) Rigid pavements

Figure 7.10 Actual and calibrated ACN comparison (concluded)